Surface Plasmon−Quantum Dot Coupling from Arrays of Nanoholes

Alexandre G. Brolo,*,† Shing C. Kwok,† Matthew D. Cooper,† Matthew G. Moffitt,*,† C.-W. Wang,† Reuven Gordon,‡ Jason Riordon,§ and Karen L. Kavanagh§

Department of Chemistry, University of Victoria, P.O. Box 3065, Victoria, B.C., Canada, V8W 3V6, Department of Electrical and Computer Engineering, University of Victoria, P.O. Box 3055, Victoria, B.C., Canada, V8W 3P6, and Department of Physics, Simon Fraser University, 8888 University Drive, Burnaby, B.C., Canada, V5A 1S6

Received: July 26, 2005; In Final Form: January 27, 2006

The coupling of semiconductor quantum dots (QDs) to the surface plasmon (SP) modes of nanohole arrays in a metal film was demonstrated for the first time, showing enhancement in the spontaneous emission by 2 orders of magnitude. The SP-enhanced transmission resonances of the nanohole arrays were tuned around the photoluminescence (PL) peak of polystyrene-*b*-poly(acrylic acid) (PS-*b*-PAA)-stabilized cadmium sulfide (CdS) quantum dots (QDs) in contact with the arrays. As a result the overall PL from the SP−QD system was enhanced by 2 orders of magnitude, even after excluding the enhanced transmission of the nanohole array without the QDs. The maximum enhancement occurred when the resonance from the nanohole array matched the QD PL spectrum. Time-resolved PL measurements were used to estimate the relative contribution of different physical mechanisms to the enhanced spontaneous emission. The increased spontaneous emission in the SP−QD system is promising for prospective plasmonic light-emitting devices incorporating QDs.

1. Introduction

The coupling between surface plasmons (SPs) and inorganic semiconductor emitters, such as quantum wells (QWs), quantum dots (QDs), and Si nanocrystals, has been a topic of intense recent interest[1−13] due to numerous potential device applications. QDs are more optically robust than organic fluorophores, and they present tunable (size-dependent) emission bands and greater flexibility in terms of excitation.[14] Their chemical behavior can also be easily manipulated by modifying their surface with the desired functionality.[15] Enhanced photoluminescence (PL) yield from QDs and nanowires in contact with metallic nanoparticles has been reported.[2,8] The surface plasmon (SP) resonances mediate an increase in the PL efficiency by either enhancing the local exciting field[2,16] or providing an alternative pathway to the spontaneous emission.[8,13] Gontijo et al.[5] showed that the decay rate of excitons in InGaN QWs is increased by a factor of 55 when in the proximity of an ultrathin silver layer due to the direct transfer of energy into the SP modes. However, since their system lacked an efficient antenna to transform the SP into free photons, the end result was an overall decrease in the PL efficiency.

The enhanced decay constant of the SE due to the interaction between the semiconductor QW and the SP was readily confirmed by time-resolved PL measurements in a similar system.[3] Enhanced PL emission was later recorded when the SP−photon conversion was induced by either coating the metal surface with Ag nanoparticles[4] or using a silver film with a rough surface.[9] In all these cases, however, random metallic structures were used to convert the SP into free photons. Hence, although an overall enhancement was obtained, tuning the enhancement to favor certain emitted frequencies was not possible in those systems. Recently, Song et al. have reported a significant enhancement in the PL efficiency from CdSe/ZnS QDs in contact with a periodic array of silver nanoparticles.[16] The efficient PL emission was assigned to an enhancement in the excitation field by a combination of propagating and localized SP resonances.[16]

There has also been a lot of interest in the optical and spectroscopic properties of periodic nanohole arrays, driven by their potential application in photonic architectures.[17] When illuminated with white light, it is known that nanohole arrays support extraordinary transmission with resonances at specific frequencies, which are related to the spacing between the holes.[18] Several models have been suggested to describe this phenomenon.[19−22] Most of these invoke the role of SPs, and indicate that the extraordinary transmission occurs when the incident excitation matches the SP resonances. It has recently been found that the polarization of light transmitted through nanohole arrays is dependent on the shape of the nanoholes,[23−25] opening the door to the possibility of using these substrates as nanopolarizers and subwavelength photonic switches. The adsorption of biological species on nanohole arrays can shift the SP resonance, producing an SPR sensor that works in transmission mode.[26] The potential application of these substrates in biophotonics was further demonstrated by the observation of several enhanced spectroscopic responses, including fluorescence,[27−33] infrared absorption,[34−36] and Raman scattering.[37]

In the present paper, we describe the first example of coupling of the SE of semiconductor QDs to the SP modes from periodic nanohole arrays in a metal film. In this experiment, the PL from the QDs is emitted into the SP modes of the metal film. For certain wavelengths, these SP modes are resonant with the periodic arrangement of nanoholes, which leads to enhanced transmission of the QD PL. These are the same SP modes that allow for enhanced transmission of Bragg resonant wavelengths

* Corresponding authors. E-mail: agbrolo@uvic.ca and mmoffitt@uvic.ca.
† Department of Chemistry, University of Victoria.
‡ Department of Electrical and Computer Engineering, University of Victoria.
§ Department of Physics, Simon Fraser University.

10.1021/jp054129c CCC: $33.50
Published on Web 04/04/2006

TABLE 1: Geometric Characteristics (in nm ±5%) of the Au Nanohole Arrays Investigated

array	periodicity	diameter	fill factor (%)
A	350	86	4.7
B	400	88	3.7
C	400	88	3.7
D	430	104	4.6
E	500	114	4.1
F	550	122	3.8
G	610	118	2.9
H	650	117	2.5
I	660	131	3.1

of light through the holes; however, for the QD PL, the SP modes are directly excited at the surface of the film. The fact that the PL transmission spectrum changes to follow the resonance of the array is a main feature of this work, which allows us to measure the SE enhancement from the coupling between the QD and the SPs. By varying the periodicity of the array, it is possible to control the enhanced PL from the QDs. The different contributions to the enhancement were estimated from time-resolved PL measurements.

For the present study, block copolymer-coated CdS QDs with trap-state emission in the same spectral range as the main SP resonance of several of the arrays of nanoholes were chosen; the polystyrene brush layer surrounding each nanoparticle afforded easy deposition of transparent QD−polymer films on the nanohole arrays. Moreover, the energy separation between the laser excitation and the emission from the trap states could potentially allow for conditions where only the emission is in resonance with the plasmonic structure. The strategy here was therefore to use a fixed emitter (CdS), while varying the structure of the plasmonic substrate in order to tune the SP resonances. Experiments with different types of QDs can be envisaged and should be a natural extension of this work.

2. Experiment

2.1. Materials and Fabrication of the Nanostructures. The arrays of subwavelength holes were fabricated and imaged with use of a FEI 235 dual-beam focused ion beam and field emission scanning electron microscope. The details of the instrument setting, fabrication, cleaning, and optical characterization of the arrays are presented elsewhere.[26,37] Nine different square arrays with distinct periodicities (distances between the centers of the nanoholes) were used in this study (Table 1). The arrays were created in 100-nm-thick gold films deposited on Cr-coated (5 nm) glass by evaporation.

Films of polystyrene-*b*-poly(acrylic acid) (PS-*b*-PAA)-stabilized cadmium sulfide (CdS) QDs were used to coat the gold substrate. CdS was used as an emitter because its PL from trap states matches the SP resonances of the gold nanostructures investigated in this work. Details on the synthesis of these polymer-stabilized CdS quantum dots (PS-QD) have been published, along with their PL properties in dilute toluene solutions.[38] These composite particles consist of a CdS QD core, surrounded by an ionic surface layer of poly(cadmium acrylate) that is covalently linked to an outer brush layer of polystyrene. The glassy poly(cadmium acrylate) surface layer provides long-term stability for the composite particles through its high glass transition temperature and Cd^{2+} ionic cross-links between carboxylate groups. The polystyrene brush provides solubility in organic solvents, and acts as both a matrix and a spacer between neighboring QDs (and the QDs and the substrate) in cast films of PS-QD. On the basis of the molecular weight of the polystyrene brush chains (34 000 g mol^{-1}) and measured

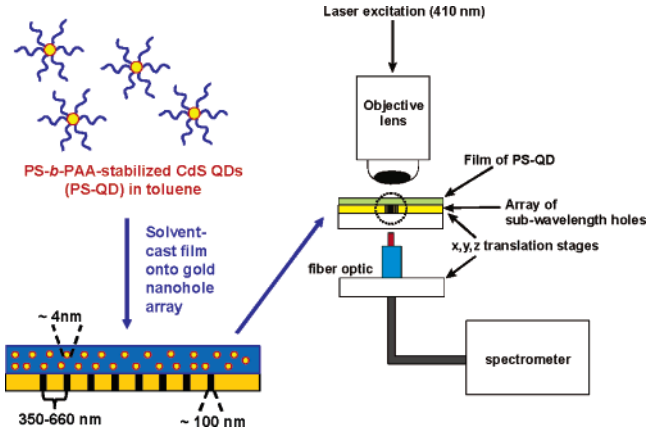

Figure 1. Schematic of the sample preparation and experimental setup. QDs inside the nanoholes are not represented.

chain aggregation numbers for a similar block copolymer-stabilized CdS sample in toluene, the calculated average nearest-neighbor distance between QDs in the polystyrene matrix of the cast films is ∼30 nm. Without micelle distortion, the calculated average distance between the first layer of QDs and the nanostructured gold substrates would be half this value (∼15 nm), although horizontal distortions due to micelle interactions with the substrate should reduce this average distance significantly.[39] Along with the prevention of QD aggregation with casting and providing uniform and optically transparent films, the polystyrene brush spacer should in the future provide fine control over the interactions between QDs and between QDs and the substrate, since QD samples with polystyrene brush chains of variable length can be prepared.

A solution of PS-QD in toluene was drop-coated on the top of various gold arrays, using a fixed volume of 20 μL. A film of the colloidal QDs dispersed in a polystyrene matrix was formed after the solvent evaporated. Since all arrays were on the same gold slide and the distance between then were less than 1 mm, we can assume a homogeneous film thickness and the same amount of PS-QDs on each array. Although a small difference in the absolute amount of PS-QDs could arise because the density of holes illuminated by the laser source is array dependent, this contribution is not significant due to the small volume of the holes (ca. 100 nm diameter and 100 nm deep) compared to the overall film thickness. Several initial concentrations of PS-QD in toluene were used, ranging from 3% to 11% w/w. The more concentrated solutions yielded thicker films, but the spacing between the dots was constant and dictated by the aggregation number and characteristic length of the polystyrene brush.[38] Experiments with normal glass slides (without gold) coated with a film of PS-QD were also performed to provide a baseline for the optical measurements.

2.2. Optical Setup for Transmission and PL Measurements. An Olympus BHSM metallurgical microscope coupled to an Ocean Optics USB-2000 miniature fiber optic spectrometer was used. All optical measurements were carried out in a collinear geometry, as shown in Figure 1, using a 100× objective lens (NA = 0.95). The halogen lamp from the microscope was the light source for the transmission measurements.[26] The acquisition time was 200 ms and 20 accumulations were recorded. For the PL measurements, the broad-band halogen lamp was substituted by a laser source. In this case, a mode-locked Ti:Sapphire, pumped by a Coherent Innova 400-15 Ar+ ion laser was used. The repetition rate was approximately 5 MHz, the nominal pulse duration was 200 fs and the pulse energy was on the order of 10 nJ. The 820 nm output

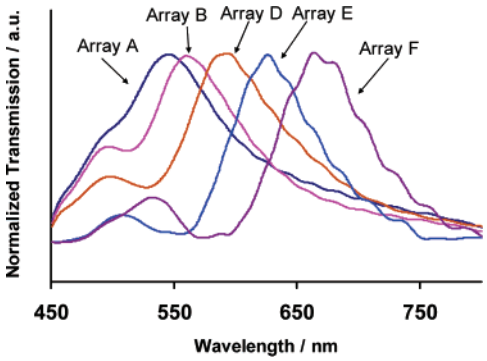

Figure 2. Normalized white light transmission for uncoated arrays of nanoholes. The geometric properties of the arrays are described in Table 1.

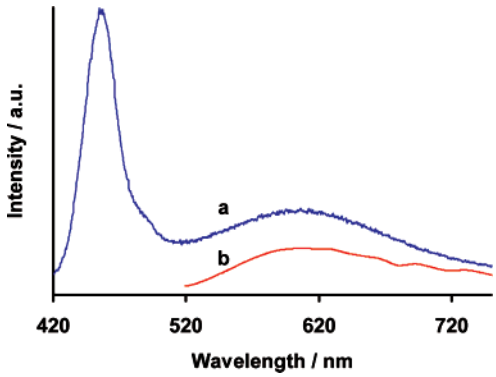

Figure 3. PL spectra of block-copolymer-stabilized CdS QDs: (a) in toluene solution and (b) film immobilized on a glass slide. Excitation at 410 nm.

of the Mira 900F oscillator was frequency-doubled, using a β-barium borate (BBO) nonlinear optical crystal mounted in a customized housing. The resulting 410 nm laser excitation was isolated by using a concentrated $CuSO_4$ solution as an optical filter, and then directed into the microscope.

For lifetime measurements, the generated PL was also collected by the optical fiber using the same arrangement, but the output was directed to a single photon counting photomultiplier system (Products for Research). The laser line was rejected by using an interference filter and the integrated PL signal was sent into the detection system. The time-dependent PL curves were deconvoluted from the instrument response function and fitted to multiexponential decays with FAST software (Alango Scientific). After the experiments, the original slide containing the arrays of subwavelength holes was regenerated by dissolving the film of PS-QD with toluene.

3. Results and Discussion

3.1. Optical Characterization of the Arrays and PL Characteristics of the QDs. The main geometrical characteristics of the arrays used in this work are summarized in Table 1. The fill factor is the relative surface area occupied by the nanoholes. The normalized transmission of white light through all arrays (without any coating) was obtained, and a representative set is shown in Figure 2. All the arrays presented extraordinary transmission at characteristic wavelengths according to their periodicity and the optical properties at the metal−air interface.[18,40] The main peak for each array in Figure 2 corresponds to the (1,0) SP resonance at the Au−air interface. The (1,0) SP mode for the Au−glass interface is not observed at longer wavelengths since this resonance is known to be attenuated by the 5 nm Cr layer between the Au and the glass slide.[20] The Au−air (1,0) SP resonance shifted to the red as the periodicity increased. This behavior is expected from the phase matching conditions for SP excitation of periodic metallic nanostructures.[41,42]

The PL spectra from a solution of the PS-QD in toluene and from a drop-coated film on a glass slide are presented in Figure 3. The PL spectrum from PS-QD dispersed in toluene (Figure 3a) presents two distinct bands: a relatively sharp peak centered at 455 nm and a broad envelop centered at 610 nm. The 455-nm peak is attributed to recombination from near-exciton band-edge states. The broad envelope at 610 nm is related to emission from a distribution of states localized at the QD surface (trap states).[38] The sharp band-edge transition is not visible in the spectrum from the films of PS-QD cast on glass (Figure 3b) because a long band-pass filter, with a cutoff at 520 nm, was used in these measurements. There are no significant differences between spectrum a and spectrum b in Figure 3 in terms of energy distribution in the trap state emission region, which indicates that the immobilization of PS-QD on glass does not affect its PL characteristics. A linear relationship was also found between the PL from various films of PS-QD on glass and the casting concentration in w/w, which is directly proportional to the film thickness. This confirms that self-quenching of the PL emission was not important for the samples investigated.

3.2. Spectral Changes in the PL Transmitted through the Arrays of Nanoholes. Figure 4 shows the white light transmission (labeled "i" in all plots) and the transmitted PL spectra (labeled "ii" in all plots) through a selected set of nanohole arrays used in this work (see Table 1 for the details regarding the arrays). Each of the arrays presented in Figure 4 was drop-coated with a 5% w/w toluene solution of PS-QD. The white light transmission, labeled "i" in Figure 4 for each array, presents distinct features when compared to Figure 2. The differences in the transmission features are related to the shift of the SP resonances due to the changes in the refractive index of the material in contact with the gold substrate.[26,40] For instance, Figure 2 shows only one Au−air resonance peak for each array, but multiple peaks are generally presented in the white light transmissions shown in Figure 4 for the PS-QD-coated arrays. The extra peaks in Figure 4 correspond to higher scattering orders of the array. A definitive assignment for the SP resonances present in Figure 4 would require the precise determination of the refractive index of the film and the application of numerical methods. However, we estimate that they are related to the (1,0) and (1,1) resonances at the Au−PS-QD interface, whereas the (1,0) mode occurs always at longer wavelength.

The white light transmission spectra of polystyrene-coated nanohole arrays in the absence of QDs were also obtained, and their main features were similar to the ones observed in Figure 4i, indicating that the presence of QDs does not significantly change the refractive index of the polymer.

The transmitted PL spectra, labeled "ii" for each array, should be compared to the reference PL from the QD film-coated glass slide presented in Figure 3b. The strong feature at 820 nm that is present in all transmitted PL spectra is the residual fundamental radiation from the laser source. A similar feature (not shown) is also observed at 410 nm, corresponding to the residual laser excitation.

It is clear from Figure 4 spectra ii that the PL spectra transmitted through the nanoholes were significantly different from the spectrum obtained from the glass slide coated with the PS-QD (presented in Figure 3b). Moreover, the PL profile was unique for each specific array, matching its characteristic

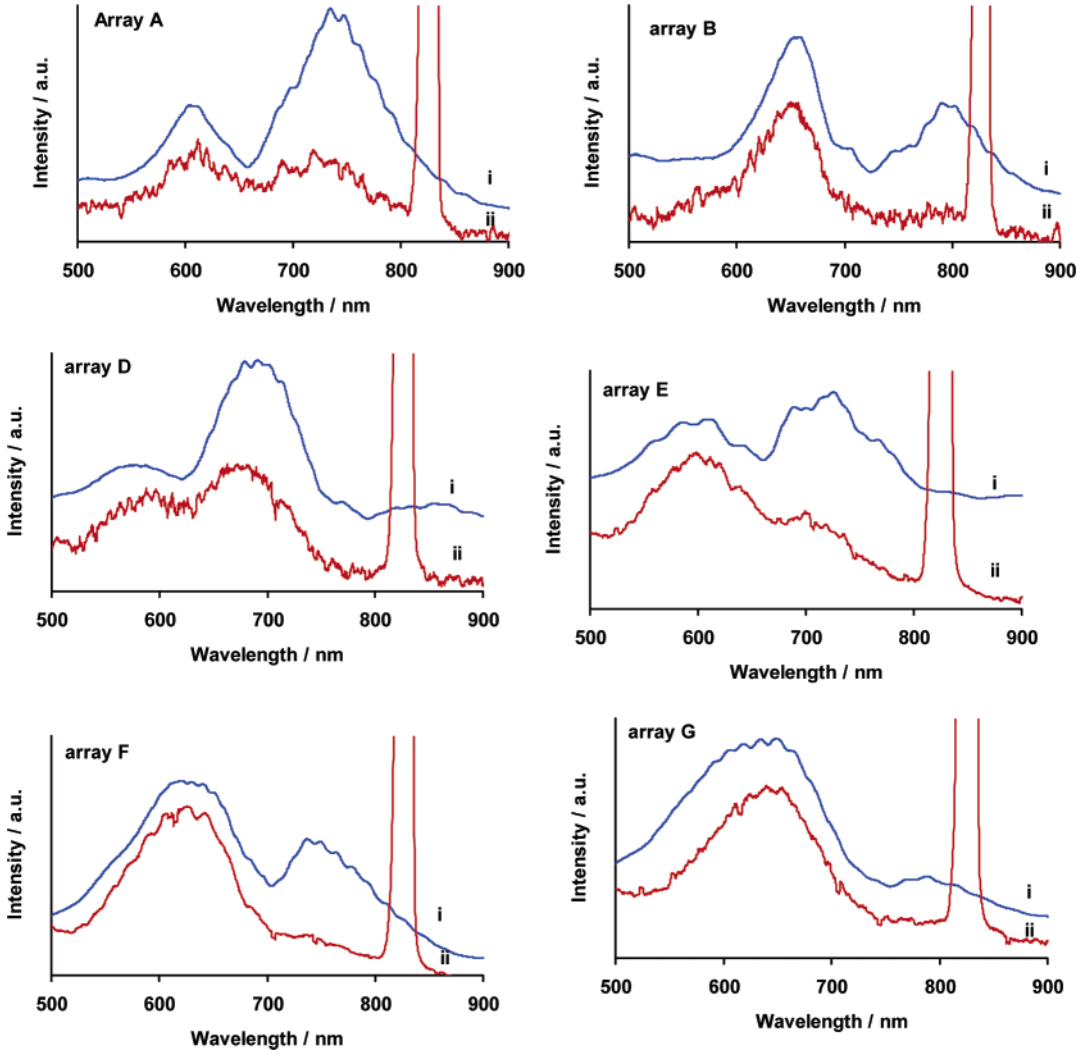

Figure 4. White light extraordinary transmission (spectra i) and transmitted PL (spectra ii) for several arrays covered with a film of block copolymer stabilized CdS QDs. Details on the geometric properties of the arrays are given in Table 1.

white light transmission. A striking feature of Figure 4 is the similarities between spectra i and ii, which illustrates that the PL is modified to follow the SP structure of the substrate. The differences in relative intensities (between i and ii in Figure 4) is related to the almost flat intensity profile of the white light source within the wavelength range investigated compared to the PL profile before transmission (shown in Figure 3). The modified PL profile reflects the fact that the SE must interact with the nanostructured gold substrate to be detected in transmission mode, and therefore the PL spectrum is combined with the SP resonances of the arrays.

The peaks in the white light transmission in Figure 4 (labeled "i" for each array) correspond to the SP resonances; hence, the array-dependent transmission PL spectrum indicates that the trap state recombination from the PS-QD excites the SP modes of the substrate. The SE from the PS−QDs located within the SP-field were either enhanced or suppressed depending on the density of accessible plasmonic states in the SE frequency range.

It is particularly interesting to point out the effect of band gaps in the plasmonic structure of the transmitted PL. When the band gap occurs within the PL range, emissions at certain wavelengths are severely attenuated creating transmitted PL spectra with double bands (see arrays A, D, and E in Figure 4). The relative intensities of these two transmitted PL bands are related to the strength of the white light transmission bands (or to the density of plasmonic states of the array). Similar plasmonic band gaps were previously reported for an organic dye adsorbed on a periodic silver grating.[43]

Investigations on QW−SP coupling[3,4] and dye−SP coupling[43] have shown that the coupling is in the weak regime, whereas J-aggregate−SP has been reported within the strong coupling regime.[44−46] Here, the QD−SP coupling appears to be in the linear regime because the observed PL has the same spectrum as the SP-enhanced transmission spectrum multiplied by the bare PL spectrum without the array.

3.3. The SP-Mediated PL Enhancement. An important aspect in plasmonics is the possibility of an enhancement in the emitter PL yield due to the SP excitations via arrays of nanoholes. Here we estimate the enhancement for the QD−SP interaction in the presence of the nanoholes. The degree of enhanced recombination rate for emitters in resonant medium is known as the Purcell effect,[47] and the Purcell factor (P) is defined as the ratio of the enhanced SE to the SE in free space.[3] While the Purcell factor is calculated from relaxation rates and lifetime measurements, or estimated from quenching measurements,[5,9] here we consider a comparable enhancement factor F as the increase in the amount of luminescent photons transmitted through the metallic nanostructure. We define the enhancement factor F as the ratio between the integrated PL transmittance (T_{PL}) and the separate measurement of the total transmittance of white light (T_{WL}) (not PL) through the arrays coated with the film of PS-QD:

$$F = \frac{T_{PL}}{T_{WL}} \quad (1)$$

Unlike other methods, no extra corrections due to fill factors and size of the nanoholes (including a correction from Bethe's theory[48]) are required, since both transmittances are measured for the same array. Other methods compare the transmission with single holes or disordered arrays.[21,30,31] Those methods are designed to demonstrate that more light than expected is transmitted through the nanoholes,[18,21] or to illustrate field localization effects.[30,31] By contrast, our objective is to probe how the overall enhancement in the QD recombination process via SP coupling results in an increase in the amount of photons produced on the other side of the array. To this end, by dividing the integrated transmittance of the PL with the total transmittance of white light, the effect of pure extraordinary transmission is eliminated.

Figure 5 shows the integrated enhancement factor (F) for all arrays, calculated with eq 1. T_{PL} was calculated from the ratio between the integrated transmitted PL intensity in the presence of the arrays (Figure 4, labeled "ii" for all arrays) and the integrated PL in the absence of the arrays (Figure 3b). T_{WL} is the total transmittance of the white light through the nanoholes coated with the QD film, calculated as the ratio between the integrated white-light spectrum transmitted through the nanoholes (Figure 4, labeled "i" for each array) and the spectrum of the light source obtained without the gold substrate (not shown).

According to Figure 5, enhanced PL was observed for all arrays investigated. The enhancement factor was dependent on the geometrical characteristics of the individual arrays and ranged from ~50 (from array A) to ~300 (from array F). It can be concluded from Figures 4 and 5 that a maximum PL efficiency is achieved when the geometrical characteristics of the arrays are designed to produce the best overlap between the SP resonance and the PL emission. Therefore, the enhancement factor depends both on the plasmonic properties of the gold substrate and on the excited states of the QDs.

The larger reflectivity of the gold surface compared to the glass was also considered, using the optical properties of Au at 410 nm.[49] Other effects, such as extra excitation due to back reflection from the polymer−air interface and SE into waveguide modes of the asymmetric cavity (metal−dielectric−air), were not considered.[50]

The values for F-factors presented in Figure 5 are comparable to typical SP-mediated enhanced recombination observed from molecular systems,[43,51−54] semiconductor QDs[2,7,10,16] and QWs.[3,5,9,12] Most of the reports, however, deal with a different situation where only the excitation field is in resonance with the SP modes.[52,55] In those cases, the enhanced emission is attributed to an increase in the local electromagnetic field at the excitation frequency.[52] In our case, however, the situation is more complex and several contributions to the total enhancement may be present. These pathways include simple radiative decays followed by photon−SP coupling, SP-mediated enhanced excitation fields, and enhanced nonradiative QD−SP coupling. The relative contributions of each of these pathways are array dependent, since the SP resonances are closely connected to the geometrical parameters of the nanostructure.

3.4. Time-Resolved PL. The relative contributions of the pathways mentioned above to the overall enhancement can be investigated from PL lifetime measurements. Figure 6 shows PL decays for the emitters in contact with the glass slide and in contact with one of the arrays of nanoholes. Similar results were obtained for other arrays. The data in each curve were fitted to multiexponential functions and the resulting fitting parameters are also given in Figure 6. The average lifetimes for the emissions through glass and through the nanoholes extracted from the fits were (282 ± 10) and (31 ± 4) ns, respectively. The lifetime decrease observed in Figure 6b is typical for emitters in contact with metallic structures. In addition, since the distance between the QDs on glass and on the gold substrates was kept constant by the polymer layer, the lifetime modification cannot be explained by dipole−dipole interaction.[38]

A lifetime distribution analysis shows that the greatest contribution to the PL decay for the film-coated array of

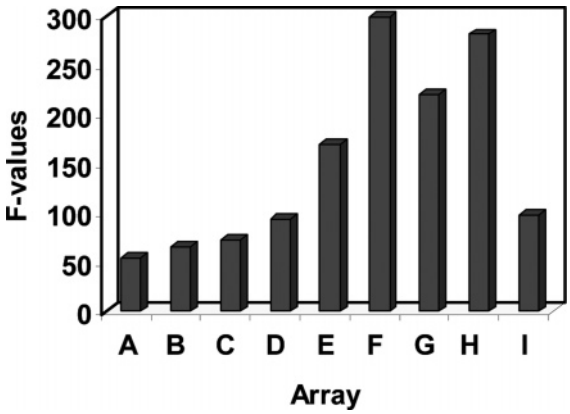

Figure 5. Enhancement factors (F-values), calculated with eq 1, for all arrays investigated.

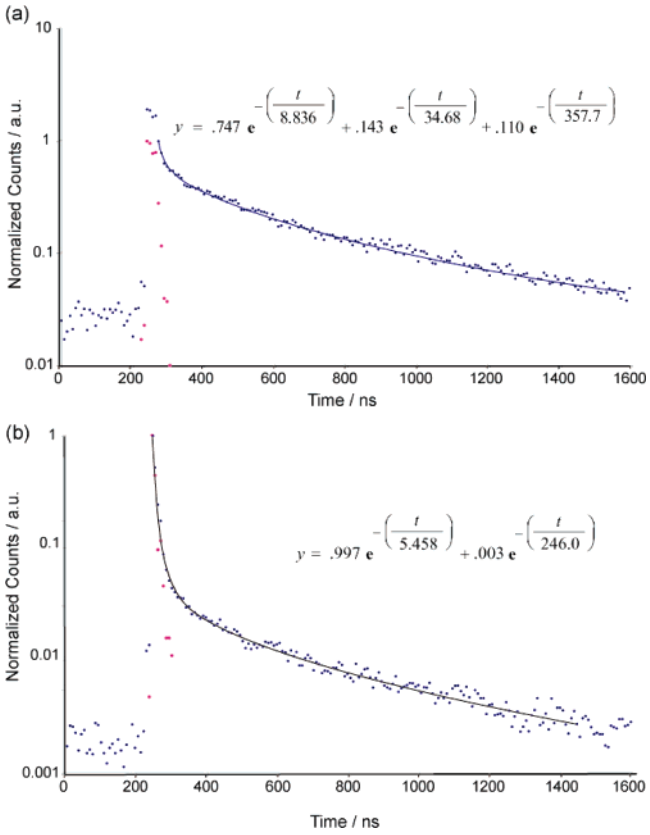

Figure 6. PL decay curves of PS-QD films: (a) on a glass slide and (b) adsorbed on an array of nanoholes (array F is presented). Triple and double exponential fittings are shown in the insets. Relative contributions of each lifetime to the total decay (obtained from the area under the exponentials): (a) τ_1 gives 13%, τ_2 gives 10%, and τ_3 gives 77% and (b) τ_1 gives 90% and τ_2 gives 10%. The red dots indicate the instrument response function (fwhm = 15 ns).

nanoholes originates from the short lifetime component of the decay curve, with the lifetime component at around 5 ns making up 90% of the PL (Figure 6b). On the other hand, the decay curve for the QD film on glass shown in Figure 6a is dominated by lifetime components at ca. 360 ns, which has a 77% contribution. The short component in Figure 6b can be assigned to the direct energy transfer from the trap states into SP excitation. A distribution of lifetimes is observed even for the polymer-coated QD films on glass due to an inhomogeneous distribution of QD states and nanoparticle sizes. Therefore, the assignment suggested above can be regarded as an approximation.

It is well accepted that the proximity of emitters to metals affects both their radiative and nonradiative rates of relaxation. For instance, Shimizu et al.[10] found a 1400 enhancement in the rate for the nonradiative process and an increase of 70 times for the radiative channel for single QDs adsorbed on rough gold surfaces. On the other hand, we may assume that the quenching occurs predominantly for QDs located close to the surface (within 10 nm), and corresponds to the direct excitation of SPs by trap recombination. Notice that, considering the thickness of the PS brush surrounding each QD, it is estimated that only a monolayer of QDs will be inside this range. The emitters outside this range will be less subject to direct SP excitation, but they will still be influenced by the SP field, which extends for hundreds of nanometers away from the surface.

It is not possible to deconvolute these effects from the multiple lifetimes obtained in Figure 6. However, assuming that the main contribution to the enhancement originates from SE quenching directly into SP modes, a Purcell factor P can be estimated from the ratio between the main contributions to the lifetimes in the presence and absence of the nanostructure. This estimation should be viewed as an upper limit for the enhancement. Hence, we have $P \approx (360\ \text{ns})/(5\ \text{ns}) \approx 72$. The estimated P-ratio for this system is similar to the ones reported for PL from QWs in the presence of silver surfaces.[3,5,9]

This increase in the SE efficiency can account for some of the F-values observed. However, it can be seen in Figure 5 that a maximum F-value of ~300 was observed for array F. Other mechanisms must therefore be operative to account for this surprisingly large enhancement. For instance, a resonance between the excitation field and nanostructure may be involved, in addition to the increase in SE decay rate described by P. Indeed, the transmittance of the laser excitation line through the array F is increased 4 times when the array is coated with the PS-QD. This increase in the transmission relative to the bare array indicates that the SP of the coated arrays is in resonance with the laser excitation, suggesting that a SP-mediated enhancement in the excitation field should also be operative in our QD PL experiments.

4. Conclusions

In summary, this work demonstrates for the first time the direct and tunable interaction between QDs and SP modes from periodic arrays of nanoholes. The transmitted PL of the PS-QD was readily modified by the SP resonances, and the PL transmitted spectrum followed the distribution of plasmonic states of the nanostructure. A linear relationship was observed between the spectral distribution of the transmitted PL and the density of plasmonic states suggesting that the interaction occurs in the weak-coupling regime. The integrated PL was also significantly enhanced (ca. 2 orders of magnitude). PL decay measurements suggest that a direct trap state recombination into SP modes combined with enhancement of the excitation field are involved in the SP−QD interaction. Therefore, a significant contribution to the overall enhancement is attributed to the recovery of energy from quenched QD states as PL photons on the other side of the arrays, which is an important advantage for this substrate when compared to other nanostructures that support SP resonances. The approach employed here is general and can be implemented for different types of emitters and used to explore pure exciton emission from passivated QDs. The distance between the particles can also be easily tuned by the length of the polymeric coat.

The results presented here should have important implications for the future development of plasmonic-based devices.[17] For instance, the SP-mediated increase in the radiative SE from QDs could yield brighter and faster light-emitting devices.[56,57] The development of plasmonic-based low-threshold and high-modulation semiconductor lasers could also benefit from the data presented here.

Acknowledgment. We gratefully acknowledge funding support for this work from NSERC, CFI, and BCKDF. This collaboration has also been facilitated by the Centre for Advanced Materials and Related Technology (CAMTEC) at the University of Victoria and by the Pacific Centre for Advanced Materials and Microstructures (PCAMM).

References and Notes

(1) Tang, J.; Birkedal, H.; McFarland, E. W.; Stucky, G. D. *Chem. Commun.* **2003**, 2278−2279.

(2) Kulakovich, O.; Strekal, N.; Yaroshevich, A.; Maskevich, S.; Gaponenko, S.; Nabiev, I.; Woggon, U.; Artemyev, M. *Nano Lett.* **2002**, *2*, 1449−1452.

(3) Neogi, A.; Lee, C. W.; Everitt, H. O.; Kuroda, T.; Tackeuchi, A.; Yablonovitch, E. *Phys. Rev. B* **2002**, *66*, 153305.

(4) Neogi, A.; Morkoc, H. *Nanotechnology* **2004**, *15*, 1252−1255.

(5) Gontijo, I.; Boroditsky, M.; Yablonovitch, E.; Keller, S.; Mishra, U. K.; DenBaars, S. P. *Phys. Rev. B* **1999**, *60*, 11564−11567.

(6) Kamat, P. V.; Shanghavi, B. *J. Phys. Chem. B* **1997**, *101*, 7675−7679.

(7) Gryczynski, I.; Malicka, J.; Jiang, W.; Fischer, H.; Chan, W. C. W.; Gryczynski, Z.; Grudzinski, W.; Lakowicz, J. R. *J. Phys. Chem. B* **2005**, *109*, 1088−1093.

(8) Lee, J.; Govorov, A. O.; Dulka, J.; Kotov, N. A. *Nano Lett.* **2004**, *4*, 2323−2330.

(9) Okamoto, K.; Niki, I.; Shvartser, A.; Narukawa, Y.; Mukai, T.; Scherer, A. *Nat. Mater.* **2004**, *3*, 601−605.

(10) Shimizu, K. T.; Woo, W. K.; Fisher, B. R.; Eisler, H. J.; Bawendi, M. G. *Phys. Rev. Lett.* **2002**, *89*, 117404.

(11) Gueroui, Z.; Libchaber, A. *Phys. Rev. Lett.* **2004**, *93*, 166104.

(12) Hecker, N. E.; Hopfel, R. A.; Sawaki, N.; Maier, T.; Strasser, G. *Appl. Phys. Lett.* **1999**, *75*, 1577−1579.

(13) Biteen, J. S.; Pacifici, D.; Lewis, N. S.; Atwater, H. A. *Nano Lett.* **2005**, *5*, 1768−1773.

(14) Alivisatos, A. P. *Science* **1996**, *271*, 933−937.

(15) Kim, S.; Bawendi, M. G. *J. Am. Chem. Soc.* **2003**, *125*, 14652−14653.

(16) Song, J. H.; Atay, T.; Shi, S. F.; Urabe, H.; Nurmikko, A. V. *Nano Lett.* **2005**, *5*, 1557−1561.

(17) Barnes, W. L.; Dereux, A.; Ebbesen, T. W. *Nature* **2003**, *424*, 824−830.

(18) Ebbesen, T. W.; Lezec, H. J.; Ghaemi, H. F.; Thio, T.; Wolff, P. A. *Nature* **1998**, *391*, 667−669.

(19) Enoch, S.; Popov, E.; Neviere, M.; Reinisch, R. *J. Opt. A*: *Pure Appl. Opt.* **2002**, *4*, S83−S87.

(20) Genet, C.; Exter, M. P. v.; Woerdman, J. P. *Opt. Commun.* **2003**, *225*, 331−336.

(21) Lezec, H. J.; Thio, T. *Opt. Express* **2004**, *12*, 3629−3651.

(22) Martin-Moreno, L.; Vidal, F. J. G.; Lezec, H. J.; Pellerin, K. M.; Thio, T.; Pendry, J. B.; Ebbesen, T. W. *Phys. Rev. Lett.* **2001**, *86*, 1114−1117.

(23) Gordon, R.; Brolo, A. G.; McKinnon, A.; Rajora, A.; Leathem, B.; Kavanagh, K. L. *Phys. Rev. Lett.* **2004**, *92*, 037401.

(24) Gordon, R.; Hughes, M.; Leathem, B.; Kavanagh, K. L.; Brolo, A. G. *Nano Lett.* **2005**, *5*, 1243−1246.

(25) Koerkamp, K. J. K.; Enoch, S.; Segerink, F. B.; Hulst, N. F. v.; Kuipers, L. *Phys. Rev. Lett.* **2004**, *92*, 183901.

(26) Brolo, A. G.; Gordon, R.; Leathem, B.; Kavanagh, K. L. *Langmuir* **2004**, *20*, 4813−4815.
(27) Garrett, S. H.; Smith, L. H.; Barnes, W. L. *J. Mod. Opt.* **2005**, *52*, 1105−1122.
(28) Brolo, A. G.; Kwok, S. C.; Moffitt, M. G.; Gordon, R.; Riordon, J.; Kavanagh, K. L. *J. Am. Chem. Soc.* **2005**, *127*, 14936−14941.
(29) Liu, Y.; Blair, S. *Opt. Lett.* **2003**, *28*, 507−509.
(30) Liu, Y.; Bishop, J.; Willians, L.; Blair, S.; Herron, J. *Nanotechnology* **2004**, *15*, 1368−1374.
(31) Liu, Y.; Blair, S. *Opt. Express* **2004**, *12*, 3686−3693.
(32) Rigneault, H.; Capoulade, J.; Dintinger, J.; Wenger, J.; Bonod, N.; Popov, E.; Ebbesen, T. W.; Lenne, P. F. *Phys. Rev. Lett.* **2005**, *95*, 117401.
(33) Wenger, J.; Lenne, P. F.; Popov, E.; Rigneault, H.; Dintinger, J.; Ebbesen, T. W. *Opt. Express* **2005**, *13*, 7035−7044.
(34) Williams, S. M.; Rodriguez, K. R.; Teeters-Kennedy, S.; Shah, S.; Rogers, T. M.; Stafford, A. D.; Coe, J. V. *Nanotechnology* **2004**, *15*, S495−S503.
(35) Williams, S. M.; Rodriguez, K. R.; Teeters-Kennedy, S.; Stafford, A. D.; Bishop, S. R.; Lincoln, U. K.; Coe, J. V. *J. Phys. Chem. B* **2004**, *108*, 11833−11837.
(36) Willians, S. M.; Stafford, A. D.; Rodriguez, K. R.; Rogers, T. M.; Coe, J. V. *J. Phys. Chem. B* **2003**, *107*, 11871−11879.
(37) Brolo, A. G.; Arctander, E.; Gordon, R.; Leathem, B.; Kavanagh, K. L. *Nano Lett.* **2004**, *4*, 2015−2018.
(38) Wang, C. W.; Moffitt, M. G. *Langmuir* **2004**, *20*, 11784−11796.
(39) Spatz, J. P.; Sheiko, S.; Moller, M. *Macromolecules* **1996**, *29*, 3220−3226.
(40) Krishnan, A.; Thio, T.; Kim, T. J.; Lezec, H. J.; Ebbesen, T. W.; Wolff, P. A.; Pendry, J.; Martin-Moreno, L.; Garcia-Vidal, F. J. *Opt. Commun.* **2001**, *200*, 1−7.
(41) Barnes, W. L.; Preist, T. W.; Kitson, S. C.; Sambles, J. R.; Cotter, N. P. K.; Nash, D. J. *Phys. Rev. B* **1995**, *51*, 11164−11167.
(42) Barnes, W. L.; Preist, T. W.; Kitson, S. C.; Sambles, J. R. *Phys. Rev. B* **1996**, *54*, 6227−6244.
(43) Kitson, S. C.; Barnes, W. L.; Sambles, J. R. *Phys. Rev. B* **1995**, *52*, 11441−11445.
(44) Wiederrecht, G. P.; Wurtz, G. A.; Hranisavljevic, J. *Nano Lett.* **2004**, *4*, 2121−2125.
(45) Bellessa, J.; Bonnand, C.; Plenet, J. C.; Mugnier, J. *Phys. Rev. Lett.* **2004**, *93*, 036404.
(46) Dintinger, J.; Klein, S.; Bustos, F.; Barnes, W. L.; Ebbesen, T. W. *Phys. Rev. B* **2005**, *71*, 035425.
(47) Purcell, E. M. *Phys. Rev.* **1946**, *69*, 681−681.
(48) Bethe, H. A. *Phys. Rev.* **1944**, *66*, 163−182.
(49) Johnson, P. B.; Christy, R. W. *Phys. Rev. B* **1972**, *6*, 4370−4379.
(50) Worthing, P. T.; Amos, R. M.; Barnes, W. L. *Phys. Rev. A* **1999**, *59*, 865−872.
(51) Ritchie, G.; Burstein, E. *Phys. Rev. B* **1981**, *24*, 4843−4846.
(52) Lee, I.-Y. S.; Suzuki, H.; Ito, K.; Yasuda, Y. *J. Phys. Chem. B* **2004**, *108*, 19368−19372.
(53) Lakowicz, J. R.; Shen, Y. B.; D'Auria, S.; Malicka, J.; Fang, J. Y.; Gryczynski, Z.; Gryczynski, I. *Anal. Biochem.* **2002**, *301*, 261−277.
(54) Okamoto, T.; H'Dhili, F.; Kawata, S. *Appl. Phys. Lett.* **2004**, *85*, 3968−3970.
(55) Aroca, R.; Kovacs, G. J.; Jennings, C. A.; Loutfy, R. O.; Vincett, P. S. *Langmuir* **1988**, *4*, 518−521.
(56) Andrew, P.; Barnes, W. L. *Science* **2004**, *306*, 1002−1005.
(57) Wedge, S.; Barnes, W. L. *Opt. Express* **2004**, *12*, 3673−3685.